

Original article

Trends in the Interannual Variability of Salinity Field in the Upper 1000-Meter Layer of the Northeastern Pacific Ocean under Conditions of Modern Global Warming

I. D. Rostov ✉, E. V. Dmitrieva

*V. I. Il'ichev Pacific Oceanological Institute, Far Eastern Branch of RAS, Vladivostok,
Russian Federation*

✉ rostov@poi.dvo.ru

Abstract

Purpose. The study is purposed at determining the trends and the regional features of interannual changes in salinity and salt content in the upper 1000-m layer of the extratropical zone in the northeastern Pacific Ocean, and at analyzing their possible cause-and-effect relations with large-scale and regional processes in the ocean and the atmosphere over the last two decades of the current period of global warming.

Methods and Results. The NOAA climate data sets including the GODAS oceanographic data assimilation system in the nodes of a regular grid, as well as the data on the amount of atmospheric precipitation and the series of climate indices were used in the study. The monthly average ERA5 reanalysis data on precipitation and evaporation from the underlying surface were also applied. The methods of cluster, correlation and regression analysis, as well as the apparatus of empirical orthogonal functions were involved. The conducted research resulted in identifying the regional spatial and temporal features of the changes in salinity and salt content in the upper 1000-m water column of the study area under conditions of the current warming phase accompanied by the intensification of global and local hydrological cycles. The quantitative characteristics of the noted trends and their statistical significance were assessed.

Conclusions. The spatial distribution of evaporation-precipitation (*E-P*) difference trends demonstrates a predominant evaporation pattern over most of the water area that differs from the global trends in a hydrological cycle in the middle and high latitudes of the Northern Hemisphere, especially over the previous period. In general, a statistically significant positive trend in salt content was observed in the upper 1000 m of the water column in the northern area, whereas in other regions and on the average over the whole water area, small statistically insignificant negative trends were noted in the above-mentioned layer. The correlation relations between the changes in average annual salinity and salt content values, on the one hand, and different large-scale regional processes and climate variables, on the other hand, are most manifested through the following parameters: climate indices *NPGO*, *IPO*, *PDO* and *AD*, the first mode of *EOF* of fluctuations in the *PCI* values of evaporation-precipitation (*E-P*) difference, and the second mode of *EOF* of anomaly of the isobaric surface *AT*₅₀₀ geopotential.

Keywords: northeastern part of the Pacific Ocean, extratropical zone, climate changes, hydrological cycle, salinity, salt content, trends, regional features, climate indices, correlations

Acknowledgments: The study was carried out within the framework of the theme of state assignment of POI FEB of RAS No. 121021700346-7 “Study of the main processes which determine state and variability of oceanological characteristics of the marginal seas of Asia and the adjacent regions of the Pacific and Indian oceans”. The authors are grateful to the developers for the opportunity to use the climatic data posted on the NOAA websites.

For citation: Rostov, I.D. and Dmitrieva, E.V., 2024. Trends in the Interannual Variability of Salinity Field in the Upper 1000-Meter Layer of the Northeastern Pacific Ocean under Conditions of Modern Global Warming. *Physical Oceanography*, 31(3), pp. 350-363.

© 2024, I. D. Rostov, E. V. Dmitrieva

© 2024, Physical Oceanography



Introduction

Modern climate changes in various geospheres are accompanied by an intensification of the global water cycle (hydrological cycle) and significant changes in the ocean surface salinity and the salt content of its water column on the scales from regional to global [1–5]. A salinity field (S) reflects a large-scale long-term balance between various components of the surface freshwater flow, processes of horizontal advection and mixing in the ocean [5–7]. Over the open ocean away from coastal areas and high latitudes, where the influence of river flow and ice melt is limited, evaporation minus precipitation is the main factor affecting freshwater flow, which, together with dynamic processes in the ocean, leads to the ocean salinity variability [8]. The corresponding response to changes in the hydrological cycle is characterized by a significant spatiotemporal heterogeneity and can be observed in the form of areas of anomalies and trends in salinity and salt content of different values and signs both on the surface and in the water column of oceans and seas [9, 10]. Moreover, due to their small volume in relation to the surface area, the water areas of marginal seas react to changing freshwater balance characteristics more strongly than in the open ocean [7, 11]. In contrast to thermal characteristics, formation of salinity field features in different World Ocean areas has a more complex, comprehensive and ambiguous nature [7, 9, 11–15].

In the course of studies of modern changes in the thermal conditions of the North Pacific Ocean, caused by a shift in the climate regime and global warming, large-scale spatiotemporal inhomogeneities in the interannual variability of thermal characteristics of water and air were identified and estimates of their quantitative values and statistical significance at the turn of the 20th–21st centuries were given [16]. Since about 2013, following the end of the “global warming pause” [17], marine heatwaves – localized areas of extremely high ocean surface temperatures (SSTs) associated with the atmospheric conditions resulting from disruption of the Earth’s energy balance [17, 18], have become common in the northeastern Pacific Ocean. In 2014–2016 and 2019–2020, these areas of SST anomalies up to 2.5–3 °C spread along the west coast of North America and much of the northeastern Pacific Ocean forming three-dimensional thermal structures that cover the upper ocean layer several hundred meters thick and persist for a long time [19]. During the past 20-year period at the beginning of the 21st century, the northeastern extratropical Pacific region generally experienced higher rates of warming (SST) compared to the previous period, while the adjacent northwestern region experienced the opposite trend [16]. Recent studies [20] enabled to identify and characterize regional spatiotemporal features of accelerated changes in salinity and water column salinity of the upper 1000 m of the northwestern Pacific Ocean in the first decades of the 21st century, accompanied by the intensification of global and local hydrological cycles. It was shown that statistically significant negative trends in the evaporation-precipitation difference were observed throughout the entire area, corresponding to the increasing trends in the humidification regime at the ocean surface. During this period, there were also significant changes in various indicators of atmospheric and ocean circulation accompanied by increased water exchange in the extratropical zone of the ocean with adjacent regions. It led to the formation of vast volumes of water columns subject to both desalination and salinization, as well as subsequent transformation. In general, in the water area of

the extratropical zone of the northwestern Pacific Ocean, there was a tendency for a gradual decrease in average salinity values at the surface and desalination of waters in the upper 1000-meter layer [5, 10].

It is of interest to consider the regional features of the interannual variability of the spatial structure of the water column salinity field and salt content of the upper 1000-meter layer of the northeastern Pacific Ocean and to compare the results obtained with the corresponding characteristics for adjacent regions. It will enable to clarify more general similar estimates previously made for the World Ocean in general [5, 9, 10].

The present paper is aimed at trends and regional features of interannual changes in salinity and salt content in the upper 1000-m layer of the extratropical zone in the northeastern Pacific Ocean and at analyzing their possible cause-and-effect relations with large-scale and regional processes in the ocean and atmosphere at the beginning of the 21st century.

Data and methods

As in the previous work [20], the data on salinity and current speed of the GODAS oceanographic observation assimilation system at $0.3^\circ \times 1^\circ$ grid points from <https://www.esrl.noaa.gov/psd/data/gridded/data.godas.html> for 2000–2022 were used. The monthly average precipitation (P) data from the ERA5 reanalysis on a $0.25^\circ \times 0.25^\circ$ grid from http://apdrc.soest.hawaii.edu/erddap/griddap/hawaii_soest_d124_2bb9_c935.html and evaporation (E) from the underlying surface WHOI OAFflux version3 on a $1^\circ \times 1^\circ$ grid (http://apdrc.soest.hawaii.edu/erddap/griddap/hawaii_soest_6b5a_df06_3eeb.html?page=1) was also used. With the help of these data, the $E-P$ difference at the nodes of a one-degree grid was calculated.

The reanalysis data of pressure fields and series of climate (circulation) indices (CI) [16]: NP , $NPGO$, PDO , SOI , PTW , IPO , WP , $NINO.WEST$ and $WPWP$ for the same years were also taken. The data listed were obtained from the NOAA websites <https://psl.noaa.gov/data/gridded/index.html> and <https://psl.noaa.gov/data/climateindices/list/>. Additionally, the Asian Depression (AD) index was calculated using the surface atmospheric pressure.

Statistics were calculated and anomaly fields of various characteristics were decomposed into principal EOF components (PC) using a unified method [16, 20]. Also, using GODAS data on salinity at 31 levels (upper level of 5 m), the values of salt content (Q_s) and their anomalies (ΔQ_s) were calculated in various layers from the surface to 1000 m depth according to the equation given in [21, p. 3520].

Based on the data averaged over the entire period of interannual changes in salinity at various levels of the upper 500-meter layer in each grid node using the cluster analysis method for the three principal EOF $S(z)$ components, four separate areas, located in different parts of the sea: northern (N), western (W), eastern (E) and southern (S) were identified (Fig. 1, *e*). Using the cluster analysis method to zonate the studied water area based on interannual fluctuations in salt content ΔQ_s in the 5–200 m layer (as was done previously for the adjacent area [20]), the results turned out to be uninformative due to excessive fragmentation of the research area.

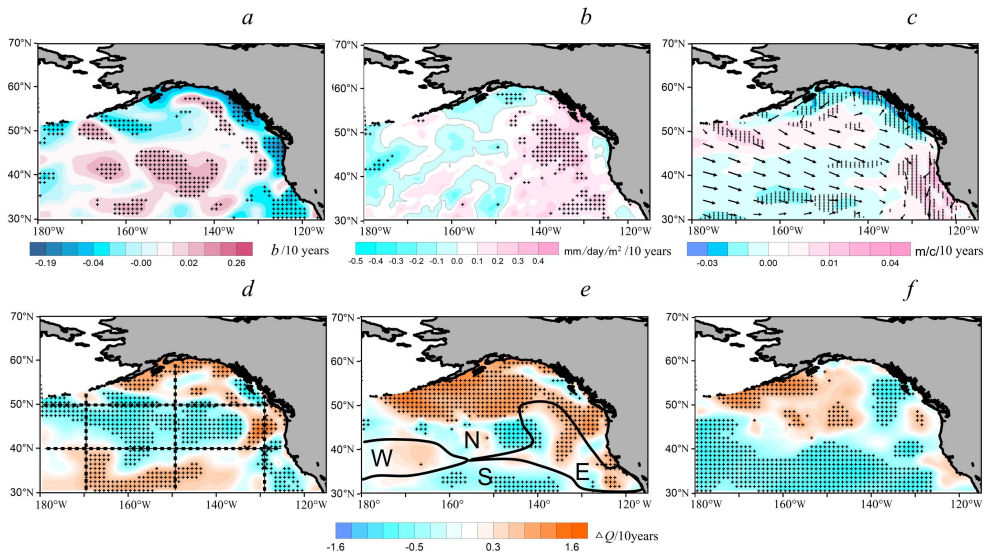


Fig. 1. Trends in average annual salinity at the 5 m level (*a*), trends in annual average values of evaporation-precipitation differences (*b*), currents (arrows) and current velocity trends (highlighted in color) at the 5 m level based on the GODAS data (*c*), trends in the normalized salt content values in the 5–200 m (*d*), 200–460 m (*e*), and 460–950 m (*f*) layers in 2000–2022. Fig. 1, *d* shows the location of sections, and Fig. 1, *e* – the location of selected regions (W, N, E and S). Here and in other figures, crosses indicate the areas where the estimates are statistically (95%) significant

Subsequently, by simple grid data averaging within the water areas of these areas, the long-term variation of salinity at each of 31 levels and salt content in individual layers was calculated: upper (5–200 m), intermediate (200–460 m) and deep (460–950 m).

Interannual spatiotemporal variability features of salinity field characteristics

In the studied water area, northern (N) and eastern (E) areas are distinguished with characteristic features inherent in the subarctic structure of waters, as well as western (W) and southern (S) ones – with features characteristic of the area of mixing waters of subarctic and subtropical structures (Fig. 1, *e*)¹ [22]. Within the entire water area, the components of the flows of the Subarctic and North Pacific currents, the Californian and Alaskan current systems can be observed [22, 23], in the interannual changes of which there are statistically significant trends in the current velocity module of different signs (Fig. 1, *c*).

During the considered period, statistically significant trends of both signs with maximum values of $-0.19 \dots 0.06/10$ years were expressed in the interannual variation of the average annual salinity at the surface level of 5 m. The areas with maximum negative salinity trends are located on the studied area periphery – in the areas adjacent to the North American continent and the Aleutian Islands. These

¹ Dobrovolsky, A.D., ed., 1968. *Pacific Ocean. Volume II. The Pacific Ocean Hydrology*. Moscow: Nauka, 524 p. (in Russian).

areas of coastal waters are affected by changes in continental runoff and water exchange with the Bering Sea. On average for the studied region, there was a tendency for a slight salinity increase at this level, in contrast to the area of the northwestern Pacific Ocean, where significant negative salinity trends were observed [20]. All areas with positive and negative salinity trends (Fig. 1, *a*) are expressed in the water area both in the warm and cold periods of the year.

At the 200 m level of the lower boundary of the upper layer, statistically significant trends in the average annual salinity of both signs were expressed with maximum values of $-0.03 \dots 0.14/10$ years at the 500 m depth – up to $-0.03 \dots 0.05/10$ years. At the same time, in the lower part of the deep layer, only small statistically significant negative salinity gradients up to $-0.02/10$ years were observed at the levels located deeper than 900 m throughout the entire water area of the northeastern Pacific Ocean.

In general, for the study area, statistically significant trends in interannual fluctuations in the average annual amount of precipitation and evaporation – indicators of the humidification regime of the underlying surface – are not expressed. Averaged over the entire water area, the maximum positive trend in both precipitation and evaporation (~ 0.04 mm/day/m² for 10 years) was expressed in the warm period of the year. These results are consistent with similar precipitation estimates obtained from <https://psl.noaa.gov/data/gridded/data.cmap.html> on a $2.5^\circ \times 2.5^\circ$ grid. The spatial distribution of trends in the evaporation-precipitation difference (*E-P*) demonstrates the predominant influence of evaporation over most of the water area, which is statistically significant in its eastern part (Fig. 1, *b*). It does not agree with the distribution of salinity trends at the ocean surface and salinity content in different layers (Fig. 1, *a, d-f*) and does not correspond to the general global trends of the hydrological cycle in the middle and high latitudes of the Northern Hemisphere [5, 7, 9], especially for the previous period of 1950–2000². As noted earlier [5, 20], in contrast to long-term changes in the characteristics of the ocean surface salinity and humidification on a global scale [10], in the middle and high latitudes, trends in spatial changes in the *E-P* difference may not be consistent with the corresponding regional trends in changes in salinity, since ocean dynamics and local factors can also play a controlling role in salinity changes on the surface and in the ocean water column ensuring a regional balance of the salinity field [9].

The patterns of spatial features of interannual changes in salt content (*Q_s*) trends in the upper, intermediate and deep layers differ significantly (Fig. 1, *d-f*), as was noted for the adjacent area of the northwestern part of the extratropical zone [20]. At the same time, the patterns of spatial distribution of salt content trends in the upper and intermediate layers in the warm and cold periods of the year do not show noticeable differences.

² Stocker, T.F., Qin, D., Plattner, G.-K., Tignor, M., Allen, S.K., Boschung, J., Nauels, A., Xia, Y., Bex, V. and Midgley, P.M., eds., 2014. *Climate Change 2013 – The Physical Science Basis: Working Group I Contribution to the Fifth Assessment Report of the Intergovernmental Panel on Climate Change*. Cambridge, United Kingdom: Cambridge University Press, 1535 p. doi:10.1017/CBO9781107415324

Note that the structures of the patterns of spatial distribution of salt content in the deep layer are in good agreement with each other in both northeastern and northwestern areas [20], where a clear zonal orientation of the boundary ($\sim 40\text{--}45^\circ\text{N}$) of large-scale areas with the opposite sign of salt content trends is observed. The noted trends in the salinity and salt content decrease in the deep layer under the conditions of intensification of the global hydrological cycle are consistent with the results of other researchers [7, 9, 10]. At the same time, vast areas can be traced within each of the layers, where over the past two decades either desalination or salinization of the water column has occurred at different velocities. On average, a velocity of $-1.4 \dots 0.8 \text{ kg/m}^2/10$ years can be observed over the water area (Fig. 1, *d–f*, Table 1).

Table 1

Estimates of the linear trend of salt content (Q_s , $\text{kg/m}^2/10$ years) of various layers of the water column in the identified areas and the entire water area in 2000–2022

Regions	Layer boundaries, m			
	5-200	200-460	460-950	5-950
N	-0.33	1.85	0.28	0.60
W	0.74	0.66	-2.40	-0.33
E	-0.38	0.55	-0.80	-0.21
S	3.12	-1.04	-2.83	-0.25
Average over the entire water area	0.79	0.51	-1.44	-0.05

Note. Here and in Table 2, statistically significant (95%) estimates are highlighted in bold.

Generalization for the water areas of individual regions: the greatest significant positive trends in salinity are observed in the upper layer of the southern region ($3.12 \text{ kg/m}^2/10$ years) and in the intermediate layer of the northern region ($1.85 \text{ kg/m}^2/10$ years); the greatest significant negative trends ($-2.83 \text{ kg/m}^2/10$ years) are in the deep layer of the southern region. In general, for the region, a statistically significant positive trend in salt content was observed in the upper ~ 1000 -meter water column of the northern region, while in other areas and on average for the water area, small statistically insignificant negative trends were observed in this layer (Table 1). These estimates of tendencies, trends and regional features of interannual changes in the salinity field structure enable to detail previously obtained estimates of changes occurring on a global scale under the conditions of the hydrological cycle intensification [1, 7, 9, 10].

As in the adjacent region of the northwestern Pacific Ocean [20], the main features of the spatial structure of trends in the salinity content of the upper layer (Fig. 1, *d*) are in good agreement with the distribution scheme of the coefficients of the first mode *EOF1* of this layer Q_s anomaly decomposition, which makes it possible to use the principal component (*PC1*) of this method of parameterizing Q_s fluctuations to establish correlations with various climate parameters.

Interannual variability of the vertical structure of salinity in the upper 1000-m layer

Formation and variability of the vertical structure of a salinity field takes place as a result of a continuous interaction of various processes on the surface, vertical

mixing and intra-water exchange. Fig. 2 shows average profiles of the vertical distribution of salinity $S(z)$, amplitude structure of $S(z)$ anomaly fluctuations – the principal EOF component $PC1$ and salinity trends $b(z)$ at various levels within the selected areas according to the data of interannual variability $S(z)$ for 2000–2022.

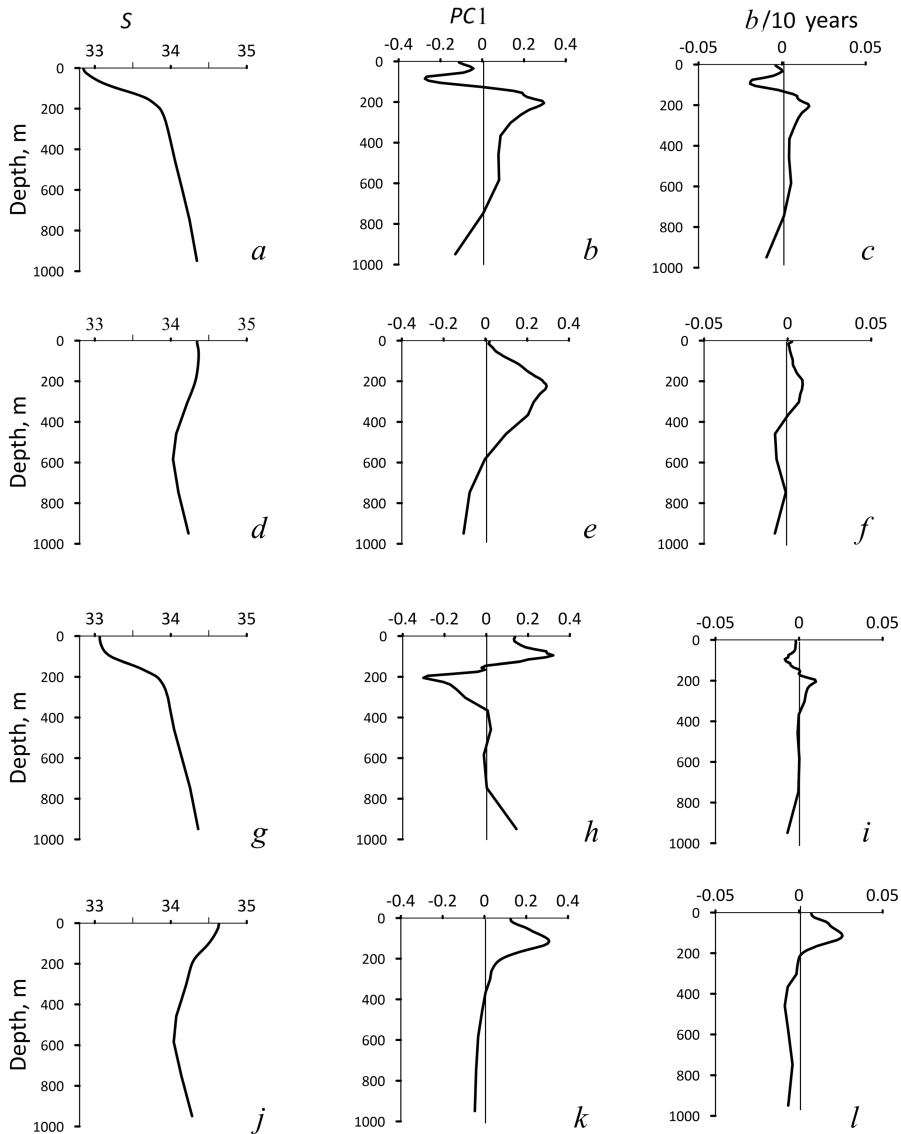


Fig. 2. Generalized curves of vertical distribution of salinity (*a, d, g, j*), principal component $PC1$ of EOF of salinity anomalies (*b, e, h, k*) and salinity trend (b) at different levels (*c, f, i, l*) for 2000–2022. From top to bottom: the N, W, E and S areas according to Fig. 1, *e*

As noted above, the features of the vertical structure of salinity in *N* and *E* areas are specific for the subarctic structure of waters with a monotonic increase in S with depth (Fig. 2, *a, g*), and in *W* and *S* areas – for the area of mixing waters of subarctic

and subtropical structures with a non-monotonic change salinity (Fig. 2, *d, j*) [22]. The $PC1(z)$ curves (Fig. 2, *b, e, h, k*) approximately correspond to the vertical distribution of the values of the range of its changes in the interannual variation (up to 0.07–0.09 in the upper 200-meter layer of the western and southern areas) and vertical distribution of salinity trends $b(z)$ in all areas (Fig. 2, *c, f, i, l*). The correlation coefficient (R) of fluctuations $PC1(z)$ and $b(z)$ is statistically significant and amounts to ± 0.84 – 0.98 . In general, the principal component $PC1$ of the interannual variability of salinity profiles in the studied areas accounts for 43% (area *E*) to 63–83% (for other areas) of the total salinity variance at different levels.

The analysis of interannual trends of statistically significant changes in the vertical structure of salinity on average for individual areas showed that the maximum negative trends ($-0.02/10$ years) were observed in the northern region (Fig. 2, *c*), and the maximum positive ones ($0.03/10$ years) – in the southern region (Fig. 2, *l*), in the layer of the upper halocline. The indicators of general trends in large-scale interannual changes in the salinity field of the studied region are the characteristics of the salinity content of the water column. According to the data in Table 1 and Fig. 1, *d–f*, within the extratropical zone of the northeastern part of the Pacific Ocean, trends in both salinization and desalination of waters in the upper, intermediate and deep layers of individual areas have prevailed in recent decades. However, in contrast to the northwestern sector of this zone [20], no statistically significant trends in salt content indicating trends in salinization or desalination of the water column of the upper 1000-m layer of the entire northeastern sector were identified. The increase in trends in the heat content of this layer of the extratropical zone of the northeastern Pacific Ocean ($\sim 2\%$) [24] was also statistically insignificant.

The spatial features of the vertical structure of the water column with different values of desalination and salinization trends are displayed on zonal and meridional sections crossing the water area of the region (Fig. 3). Over most of the area in the plane of all sections, statistically significant salinity trends of different values and signs are expressed forming the structures of large-scale salinity anomalies in various water column layers (Fig. 1, *d–f*).

The southern zonal section along 40°N crosses the western and eastern areas and the southern part of the northern one (Fig. 3, *a; 1, d*). The greatest positive salinity trends up to 0.02 – $0.03/10$ years can be seen in the upper 30-meter layer in this section center and in the 120–220 m layer in its eastern part; the greatest negative trends up to $-0.07/10$ years are observed in the upper 100-meter layer off the North American coast influenced by continental runoff and upwelling [22].

The formation of trends in interannual changes in salinity on the northern zonal section (Fig. 3, *b; 1, d*), in contrast to the southern one, takes place in the absence of noticeable horizontal latitudinal gradients in the spatial distribution of salinity within the entire 1000-meter layer. In the lower part of the upper 150-meter layer of the western part of the section, negative salinity trends with maximum values of up to $-0.08/10$ years prevail in this layer. In the upper part of the 150-meter layer in the western and eastern parts of the section at 50°N , local areas with positive S trends

are observed. The position of these areas is consistent with the horizontal distribution pattern of the $E-P$ difference values (Fig. 1, *b*). In the layer of 150–600 m over most of the section, positive salinity trends are expressed with a maximum value at the 200 m level of up to 0.02–0.04/10 years, and below it, the trend sign changes to the opposite again. The results obtained enable to detail general regional features of the interannual variability of the vertical structure of a salinity field in the northern area (Fig. 2, *c*) and others.

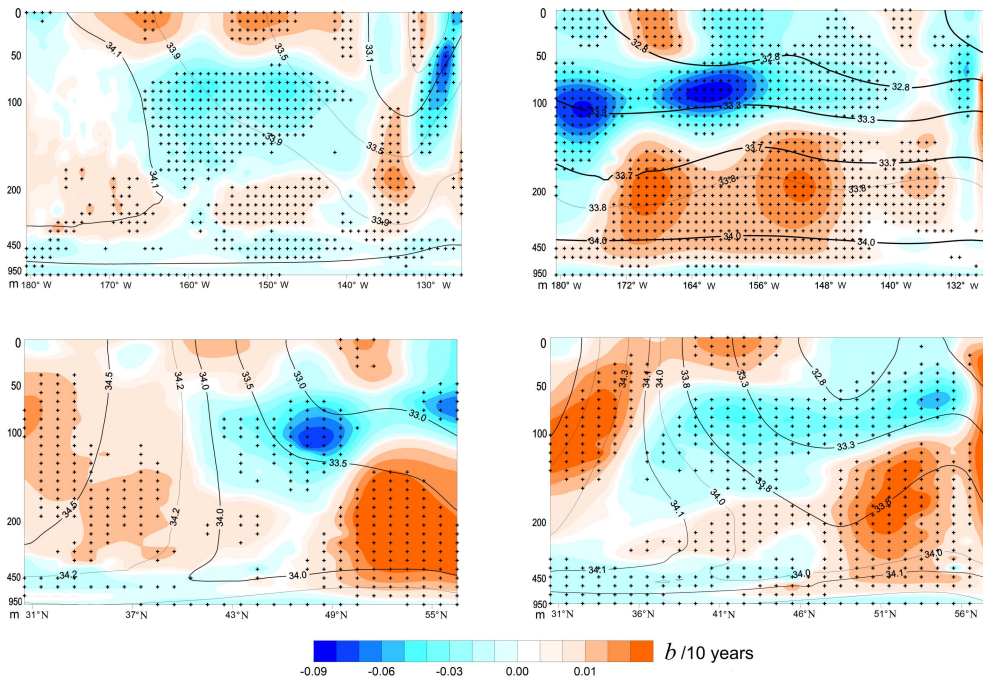


Fig. 3. Combined vertical distribution of salinity (solid lines) and salinity trends (highlighted in color) on the zonal sections along 40°N (*a*) and 50°N (*b*), and on the meridional sections along 170°W (*c*) and 150°W (*d*) in 2000–2022. Section locations are shown in Fig. 1, *d*

Formation of trends in interannual changes in salinity on meridional sections at 170°, 150° and 130°W (no Figure) occurs under the conditions of significant spatial gradients of the salinity field (Fig. 3, *c*, *d*; 1, *d*). Note that the maximum negative salinity trends with values up to $-0.07/10$ years were localized at levels of 70 and 120 m in the northern part of the western section (170°W) near the Aleutian island ridge. Areas with maximum values of positive trends S (0.06/10 years) can be observed in various parts of the upper and intermediate layers in all sections under consideration, where they are elongated in the latitudinal direction.

The analysis of maps of interannual variability of currents at 105 and 205 m levels, constructed according to GODAS data, showed that anomalous extremes of positive and negative salinity trends located near these levels correspond to the areas of localization of statistically significant trends in the current velocity module with a value exceeding ± 0.03 m/s/10 years.

Trends in the vertical and horizontal structure variability of the salinity field are reflected in the corresponding changes in the characteristics of the salinity of different water column layers (Fig. 1, *d–f*). Note that the values of salinity trends in the water column of the studied area are approximately 2–10 times (depending on the sign) less than in the northwestern part of the extratropical zone of the Pacific Ocean [20], which lies in the same climatic zone.

Correlations of interannual changes in characteristics of a salinity field with large-scale and regional processes in the ocean and atmosphere

A mutual correlation and regression analysis of interannual variations in the time series of salinity and time coefficients of the first (*PC1*) and second (*PC2*) *EOF* decomposition modes of *Qs* anomalies in the upper and intermediate layers of the water column with changes in climate indices and other indicators characterizing the dynamics of the atmosphere and ocean climate system, as well as the humidification regime in the studied region was carried out. The main characteristics of these climatic variables and their temporal variability have already been considered by the authors in the previous works [20, 24]

In the region overall, correlations between the changes in the average annual salt content values *Qs* and its principal components *PC1* and *PC2* with various climatic variables are most pronounced with the following parameters: *NPGO* indices (with a time lag of 1 year), *IPO*, *PDO* and *AD*, the first mode of *EOF* fluctuations in difference evaporation-precipitation (*E-P*) values and the second *EOF* mode of the geopotential isobaric surface *AT*₅₀₀ anomaly (Table 2).

Table 2

**Correlation coefficients of principal components and annual average salt
content values (*Qs*) in the 5–200 m and 200–460 m layers with climatic indices
for different regions for 2000–2022**

Components and regions	Parameters					
	<i>NPGO</i>	<i>IPO</i>	<i>PC1(E-P)</i>	<i>PC2(ΔAT₅₀₀)</i>	<i>PDO</i>	<i>AD</i>
5–200 m layer						
<i>PC1</i>	0.7	0.2	-0.4	-0.6	0.5	0.5
<i>PC2</i>	0.8	-0.5	0.4	0.3	-0.6	-0.6
N	0.2	-0.2	0.3	0.0	-0.3	-0.4
W	0.1	-0.4	0.5	0.5	-0.5	-0.5
E	0.5	-0.2	0.0	-0.2	-0.3	-0.3
S	-0.5	-0.6	0.5	0.7	-0.6	-0.6
Entire water area	-0.2	-0.6	0.6	0.6	-0.8	-0.8
200–460 m layer						
<i>PC1</i>	-0.6	0.1	0.0	0.0	0.2	0.1
<i>PC2</i>	-0.3	-0.4	0.5	0.5	-0.4	-0.5
N	-0.6	-0.1	0.2	0.2	-0.1	-0.2
W	0.2	-0.4	0.5	0.2	-0.5	-0.4
E	-0.6	0.0	0.4	0.3	-0.1	-0.2
S	0.3	-0.2	0.3	0.1	-0.3	-0.3
Entire water area	0.0	0.4	0.6	0.3	-0.5	-0.6

Interannual changes in some of these variables are interrelated, which leads to the identity of corresponding estimates of the correlation coefficients given in Table 2 (5–200 m layer) for pairs of variables $PC1(E-P) - PC2(\Delta AT_{500})$, $PDO - AD$. As in other areas [20], the closeness of correlations between the variability of climatic parameters, salinity and salt content fades with depth.

The maps of spatial distribution of paired regression coefficients (Fig. 4) provide visual representation of the nature of spatial features and closeness of correlations between salt content changes and the most important climatic parameters in different areas. Moreover, the corresponding schemes for each of the pairs of variables discussed above are similar. Taking into account different signs of correlation coefficients (Table 2), these features (Fig. 4, *a – c*) are in good agreement with the distribution patterns of salt content trends in the upper layer (Fig. 1, *d*).

Explained variance (R^2) of multiple regression of $PC1(Qs)$ variability of the upper 5–200 m layer and climate variables $NPGO$, $PC1(E-P)$, $PC2(\Delta H_{500})$ and PDO during 2000–2022 was 60%, i.e. the combination of these variables satisfactorily describes the observed changes in the main salt content component (Fig. 4, *d*).

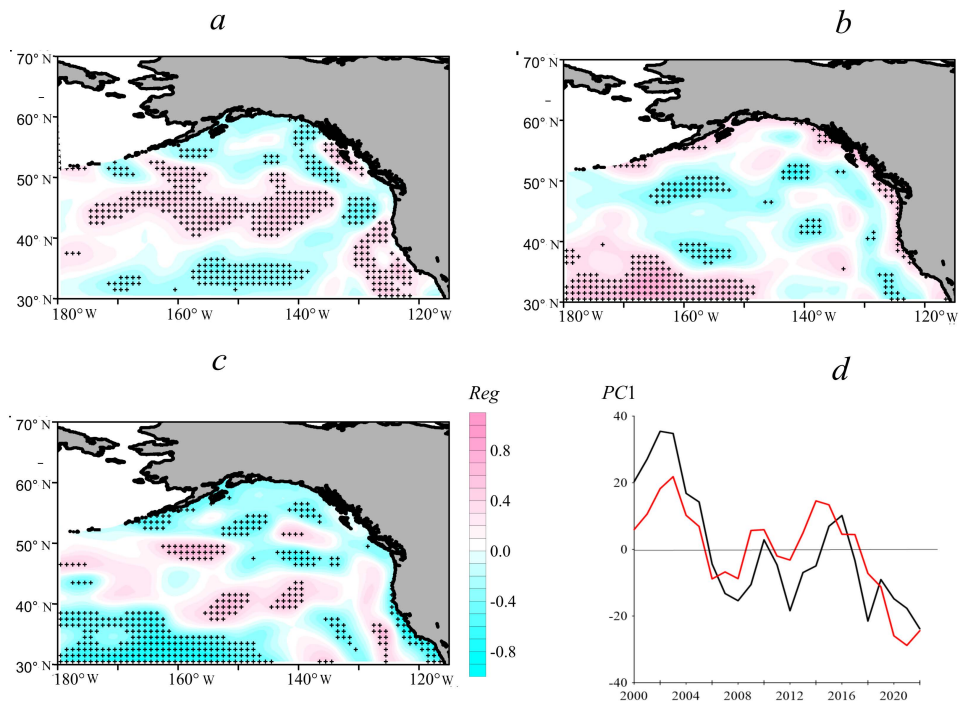


Fig. 4. Linear regression coefficients (Reg) of the fluctuations of average annual salinity anomaly values in the upper 5–200 m layer with $NPGO$ (*a*), $PC1$ of evaporation-precipitation difference (*b*) and PDO (*c*) in 2000–2022; interannual changes in $PC1(Qs)$ of the upper layer (black curve), and fitting curve of the multiple regression equation (shown in red) with different climatic indices (*d*)

Conclusion

Over the past two decades, the interannual salinity variation at the 5 m surface level has expressed statistically significant trends of both signs with maximum values of $-0.19 \dots 0.06/10$ years. On average for the considered area, there was a tendency for a slight increase in the average salinity at this level, in contrast to the northwestern Pacific Ocean area, where significant negative salinity trends were observed. The trend values decrease with depth. In general, these values in the water column of the studied area are approximately 2–10 times (depending on the sign) less than in the northwestern part of the extratropical zone of the Pacific Ocean, which is in the same climatic zone.

Within the considered area, statistically significant trends in interannual fluctuations in the average annual precipitation and evaporation are not expressed. At the same time, the spatial distribution of trends in evaporation-precipitation ($E-P$) difference values demonstrates a predominant evaporation pattern over most of the water area, which differs from the general global trends in the hydrological cycle in the middle and high latitudes of the Northern Hemisphere, especially over the previous period.

The patterns of spatial distributions of interannual variability in salt content trends in the upper, intermediate and deep layers differ significantly from each other. Summarized: when comparing the water areas of individual considered regions, it was found that the greatest significant positive trends in salt content were observed in the upper layer of the southern region ($3.12 \text{ kg/m}^2/10$ years) and in the intermediate layer of the northern region ($1.85 \text{ kg/m}^2/10$ years), and the greatest negative trends ($-2.83 \text{ kg/m}^2/10$ years) were in the deep layer of the southern region. In general, for the region, a statistically significant positive trend in salt content was observed in the upper 1000-meter water column of the northern region, while in other areas and on average for the water area, small statistically insignificant negative trends were observed in this layer.

Correlation relations between the changes in average annual salt content values and the principal components $PC1-2$ (Qs) with various climatic variables are most pronounced with the following parameters: climate indices $NPGO$, IPO , PDO and AD , the first mode of EOF fluctuations in $PC1$ values of the evaporation-precipitation difference ($E-P$) and the second mode of EOF geopotential anomaly of the isobaric surface AT_{500} .

REFERENCES

1. Lagerloef, G., Schmitt, R., Schanze, J. and Kao, H.-Y., 2010. The Ocean and the Global Water Cycle. *Oceanography*, 23(4), pp. 82-93. <https://doi.org/10.5670/oceanog.2010.07>
2. Zika, J.D., Skliris, N., Nurser, A.J.G., Josey, S.A., Mudryk, L., Laliberté, F. and Marsh, R., 2015. Maintenance and Broadening of the Ocean's Salinity Distribution by the Water Cycle. *Journal of Climate*, 28(24), pp. 9550-9560. <https://doi.org/10.1175/JCLI-D-15-0273.1>
3. Yu, L., Josey, S.A., Bingham, F.M. and Lee, T., 2020. Intensification of the Global Water Cycle and Evidence from Ocean Salinity: A Synthesis Review. *Annals of the New York Academy of Science*, 1472(1), pp. 76-94. <https://doi.org/10.1111/nyas.14354>
4. Liu, M., Vecchi, G., Soden, B., Yang, W. and Zhang, B., 2021. Enhanced Hydrological Cycle Increases Ocean Heat Uptake and Moderates Transient Climate Change. *Nature Climate Change*, 11(10), pp. 848-853. <https://doi.org/10.1038/s41558-021-01152-0>

5. Liu, Y., Cheng, L., Pan, Y., Abraham, J., Zhang, B., Zhu, J. and Song, J., 2022. Climatological Seasonal Variation of the Upper Ocean Salinity. *International Journal of Climatology*, 42(6), pp. 3477-3498. <https://doi.org/10.1002/joc.7428>
6. Durack, P.J. and Wijffels, S.E., 2010. Fifty-Year Trends in Global Ocean Salinities and Their Relationship to Broad-Scale Warming. *Journal of Climate*, 23(16), pp. 4342-4362. <https://doi.org/10.1175/2010JCLI3377.1>
7. Helm, K.P., Bindoff, N.L. and Church, J.A., 2010. Changes in the Global Hydrological-Cycle Inferred from Ocean Salinity. *Geophysical Research Letters*, 37(18), L18701. <https://doi.org/10.1029/2010GL044222>
8. Yu, L., 2021. A Global Relationship between the Ocean Water Cycle and Near-Surface Salinity. *Journal of Geophysical Research*, 116(C10), C10025. <https://doi.org/10.1029/2010JC006937>
9. Li, G., Zhang, Y., Xiao, J., Song, X., Abraham, J., Cheng, L. and Zhu, J., 2019. Examining the Salinity Change in the Upper Pacific Ocean during the Argo Period. *Climate Dynamics*, 53(9–10), pp. 6055-6074. <https://doi.org/10.1007/s00382-019-04912-z>
10. Skliris, N., Marsh, R., Josey, S.A., Good, S.A., Liu, C. and Allan, R.P., 2014. Salinity Changes in the World Ocean since 1950 in Relation to Changing Surface Freshwater Fluxes. *Climate Dynamics*, 43(3–4), pp. 709-736. <https://doi.org/10.1007/s00382-014-2131-7>
11. Durack, P.J., 2015. Ocean Salinity and the Global Water Cycle. *Oceanography*, 28(1), pp. 20-31. <https://doi.org/10.5670/oceanog.2015.03>
12. Cheng, L., Trenberth, K.E., Gruber, N., Abraham, J.P., Fasullo, J.T., Li, G., Mann, M.E., Zhao, X. and Zhu, J., 2020. Improved Estimates of Changes in Upper Ocean Salinity and the Hydrological Cycle. *Journal of Climate*, 33(23), pp. 10357-10381. <https://doi.org/10.1175/JCLI-D-20-0366.1>
13. Cravatte, S., Delcroix, T., Zhang, D., McPhaden, M. and Leloup, J., 2009. Observed Freshening and Warming of the Western Pacific Warm Pool. *Climate Dynamics*, 33(4), pp. 565-589. <https://doi.org/10.1007/s00382-009-0526-7>
14. Friedman, A.R., Reverdin, G., Khodri, M. and Gastineau, G., 2017. A New Record of Atlantic Sea Surface Salinity from 1896 to 2013 Reveals the Signatures of Climate Variability and Long-Term Trends. *Geophysical Research Letters*, 44(4), pp. 1866-1876. <https://doi.org/10.1002/2017GL072582>
15. Shi, H. and Du, L., 2021. The Unexpected Salinity Trend Shifts in Upper Tropical Pacific Ocean under the Global Hydrological Cycle Framework. In: EGU, 2021. *EGU General Assembly 2021*. Gottingen, 2021. EGU21-14698. <https://doi.org/10.5194/egusphere-egu21-14698>
16. Rostov, I.D. and Dmitrieva, E.V., 2021. Regional Features of Interannual Variations in Water Temperature in the Subarctic Pacific. *Russian Meteorology and Hydrology*, 46(2), pp. 106-114. <https://doi.org/10.3103/S1068373921020059>
17. Loeb, N.G., Thorsen, T.J., Norris, J.R., Wang, H. and Su, W., 2018. Changes in Earth's Energy Budget during and after the "Pause" in Global Warming: An Observational Perspective. *Climate*, 6(3), 62. <https://doi.org/10.3390/cli6030062>
18. Bond, N.A., Cronin, M.F., Freeland, H. and Mantua, N., 2015. Causes and Impacts of the 2014 Warm Anomaly in the NE Pacific. *Geophysical Research Letters*, 42(9), pp. 3414-3420. <https://doi.org/10.1002/2015GL063306>
19. Amaya, D.J., Miller, A.J., Xie, S.-P. and Kosaka, Y., 2020. Physical Drivers of the Summer 2019 North Pacific Marine Heatwave. *Nature Communications*, 11, 1903. <https://doi.org/10.1038/s41467-020-15820-w>
20. Rostov, I.D. and Dmitrieva, E.V., 2024. Interannual Salinity Changes in the Upper 1000-Meter Layer of Extratropical Zone in the Northwestern Pacific Ocean under Conditions of the Intensification of Global Hydrological Cycle. *Physical Oceanography*, 31(2), pp. 194-207.
21. Corbett, C.M., Subrahmanyam, B. and Giese, B.S., 2017. A Comparison of Sea Surface Salinity in the Equatorial Pacific Ocean during the 1997–1998, 2012–2013, and 2014–2015 ENSO Events. *Climate Dynamics*, 49(9–10), pp. 3513-3526. <https://doi.org/10.1007/s00382-017-3527-y>

22. Favorite, F., Dodimead, A.J. and Nasu, K., 1976. *Oceanography of the Subarctic Pacific Region, 1960-71*. Tokyo, Japan: Kenkyusha Printing Company, 187 p.
23. Kuroda, H., Suyama, S., Miyamoto, H., Setou, T. and Nakanowatari, T., 2021. Interdecadal Variability of the Western Subarctic Gyre in the North Pacific Ocean. *Deep Sea Research Part I: Oceanographic Research Papers*, 169, 103461. <https://doi.org/10.1016/j.dsr.2020.103461>
24. Rostov, I.D., Dmitrieva, E.V. and Rudykh, N.I., 2023. Trends and Regional Features of Variability of the Northeast Pacific Ocean Thermal Conditions North of 30°N over the Last Four Decades. *Physical Oceanography*, 30(4), pp. 410-427.

About the authors:

Igor D. Rostov, Head of the Informatics and Ocean Monitoring Laboratory, V.I. Il'ichev Pacific Oceanological Institute, Far Eastern Branch of RAS (3 Baltiyskaya Str., Vladivostok, 690041, Russian Federation), CSc (Geogr.), **ORCID ID: 0000-0001-5081-7279**, rostov@poi.dvo.ru

Elena V. Dmitrieva, Senior Research Associate, Informatics and Ocean Monitoring Laboratory, V.I. Il'ichev Pacific Oceanological Institute, Far Eastern Branch of RAS (3 Baltiyskaya Str., Vladivostok, 690041, Russian Federation), CSc (Techn.), **ORCID ID: 0000-0002-0094-5296**, e_dmitrieva@poi.dvo.ru

Contribution of the co-authors:

Igor D. Rostov – development of the article structure, processing and analysis of the data, writing the article text

Elena V. Dmitrieva – collection and processing of oceanographic data, calculations, drawing design, text editing

The authors have read and approved the final manuscript.

The authors declare that they have no conflict of interest.